Armenian Journal of Physics, 2017, vol. 10, issue 1, pp. 30-35

Numerical Analysis of Light Non-Resonant Transmission Through a Sub-Wavelength Slit at Angular Incidence

Kh. Sahakyan, Kh. Nerkararyan

Yerevan State University, 1 Alex Manoogian, 0025 Yerevan, Armenia

E-mail: khachiksah.91@gmail.com

Received 19 January 2017

Abstract. Numerical analysis revealed that the dependence of transmitted intensity through a subwavelength slit, milled in thin metal screen on the angle of incidence is divided into two different zones by the supreme angle. In the first zone, the intensity of the non-resonant extraordinary transmission is described by a weak non-monotonic curve, while a rapid decline is seen in the second zone. The supreme angle does not depend on incident wavelength, slit width, metal screen thickness or metal type, and equals to 62° for p-polarized light and 44° for s-polarized light. Independently of the structural parameters and wavelength, the distributions of transmitted wave fields are represented by the Hankel functions and are homogeneous by angle.

Keywords: Subwavelength structure, extraordinary optical transmission (EOT), wave field enhancement, periodical slit systems

1. Introduction

The past two decades gave a rise to new optical phenomena enhancing our understanding of light-media interaction processes. Metamaterials, small mode volume and high Q-factor cavities, photonic crystals are only the small amount of novel optical systems. The extraordinary transmission (EOT) through a subwavelength metallic hole arrays reported by Ebessen et. al. [1] is another example of new phenomena that inspired great interest to explore the underlying physics, develop new theories [2-6] and find out possible applications [7-12]. EOT is now confirmed for various structures such as holes, square, triangle [2- 4, 13-15], various materials including perfect electric conductors (PEC), real metals [1-2, 6, 16] and even for acoustic waves [17].

The simplest structure, where the EOT phenomenon is observed, is the subwavelength single slit, milled in a thin metallic screen. Here, the occurrence of EOT resulted in dubious conclusions and explanations. Especially, several authors [4, 18-20] consider that EOT, which is accompanied by extraordinary enhancement of wave field in the slit, is driven by the focusing of plasmon polaritons formed on the metal surface. In [21] the authors assume that the main mechanism of extraordinary enhancement of wave field in the slit is the magnetoelectric interference between the incident and evanescent wave fields. In [6] analytically was described light transmission through a single subwavelength slit in a thin perfect electric conductor screen and derived simple, yet accurate, expressions for the transmission efficiency. The following expression was obtained for the ratio of the electric field in the slit of a thin metallic screen to the incident electric field, which is in good agreement with [22]:

$$q = \frac{\lambda}{d}\frac{i}{i\pi + 2ln\frac{\lambda}{d}}, \qquad (1)$$

where λ is the incident wavelength, d is the width of the slit. Nevertheless, this expression and transmission efficiency, calculated using the expression above, describes the normal incidence case of EOT.

Dependence of EOT, explained by localized Fabry-Perot resonances, on the angle of incidence,

was analyzed in [22] and [23] for p-polarized and s-polarized waves, respectfully. As later experimentally revealed [12] and analytically described [6, 24] EOT can show non-resonant (broadband) transmission feature in the mid-infrared region and at lower frequencies.

In this paper, we numerically analyze the dependence of plane incident wave non-resonant transmission through a single slit (or slit arrays), milled in the thin metal screen, on the angle of incidence in the middle infrared region. Two most important cases are considered: 1. p-polarized wave, where the magnetic field is parallel to the metal surface and to the axis of a slit (Fig. 1a), and 2. s-polarized wave, where the electric field is parallel to the metal surface and perpendicular to the axis of the slit (Fig. 1b). It is assumed that the incident wavelength is much bigger than the slit width, which in its turn is greater than the thickness of the metal screen.

2. Structure of the problem

The structure of the model under investigation is shown in Fig. 1. A slit with width *d* is milled in a thin metal screen with thickness *t*. Air is selected as a surrounding dielectric media. We computationally analyze wave transmission through the structure using Finite-Difference Time-Domain (FDTD) method close to 5000 nm spectra while keeping the metal thickness smaller than the width of the slit. Periodic Broadband Fixed Angle Source Technique (BFAST) boundaries were selected for X min, X max, Z min and Z max boundaries of the FDTD solver to support plane wave angular incidence. The ***k*** wave vectors on the BFAST boundaries were taken to match the plane wave port angle of incidence and changed simultaneously with the incidence angle sweep. At the same time, steep angle 12 layer PMLs (Perfectly Matched Layer) were used for Y min and Y max boundaries of the FDTD solver region to effectively handle (absorb) waves falling at big incident angles. Lastly, power monitor was placed at the opposite side of the metal to record the transmitted power through the slit. p-polarized (Fig. 1a) or s-polarized (Fig. 1b) incident plane wave port was placed inside the FDTD region, a little lower than Y max boundary.

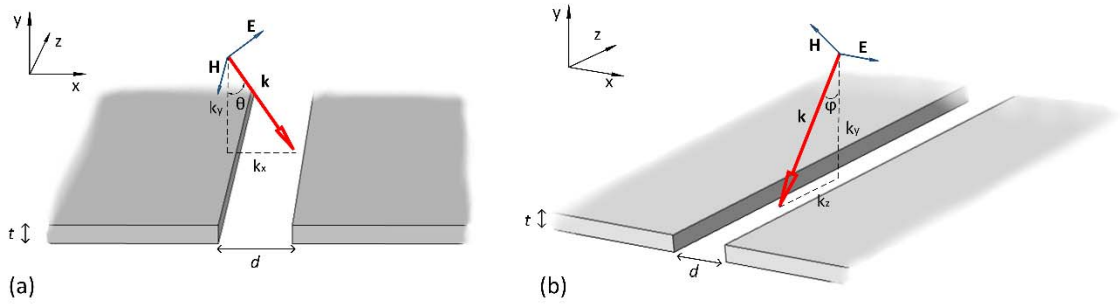

Fig.1.The geometry of the structure under study. (a) – when the wave vector of the p-polarized plane wave is in XOY plane; (b) – when the wave vector of s-polarized plane wave is in ZOY plane

FDTD method converts Maxwell's curl equations into difference equations and subsequently solves them depending on boundary conditions. For this, the computational region is divided into Yee cells having sizes of $\Delta X = \Delta Y = 50$ nm and $\Delta Z = 150$ nm. In addition, refined conformal meshing was performed for metal and slit regions to get accurate results and ensure the stability of the solution. Yee cells' sizes at these regions were selected $\Delta X = \Delta Y = 2$ nm and $\Delta Z = 5$ nm.

3. Results and discussions

We start with p-polarized incident wave, when the incident wave vector ***k*** is in the XOY plane (φ = 0°, Fig. 1a) and sweep incident angle θ from 0 to 89 degrees in order to obtain the transmitted power dependence on θ. In Fig. 2 are presented the distributions of E field for different incident angles of the p-polarized wave. As incident port is located on the upper side of the metal, constructive interference of the incident and scattered from the metal fields is seen in the upper region. This region is not informative, so we exclude it from the Fig. 2 and concentrate on transmitted E field on the lower region from the metal, near to slit. As assumed and later numerically verified in [6], at normal incidence transmitted electric field is described by Hankel function. Here, the spatial distribution of the transmitted electric field can be described by Hankel function regardless of the angle of incidence. The dependence of the transmitted power through the single slit, having the properties mentioned above, on the incident θ angle is shown in Fig. 3 (solid line).

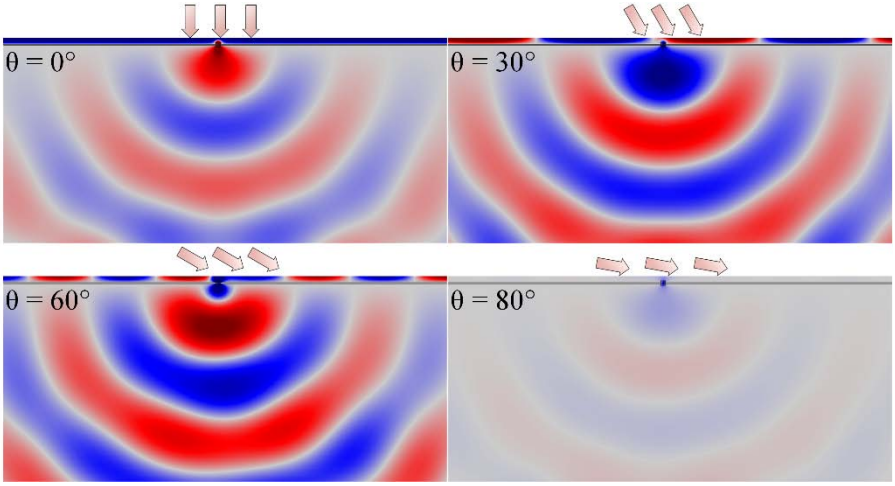

Fig 2. The electric field in a region near to a slit, at different angles of incidence of p-polarized wave for single slit, when slit width d = 100 nm, PEC screen thickness t = 50 nm and wavelength λ = 5000 nm. An incident p-polarized wave direction is presented by arrows.

Furthermore, we take Fig. 3a solid curve as a reference and analyze EOT angular dependence varying the PEC screen thickness t and slit width d. In Fig. 3(a) and (b) the transmission curve behavior stays the same for various structural parameters. The only significant difference in these curves for PEC when $t < d$ is the amount of the transmitted power at any angle, which is in good agreement with the [6] for the normal incidence case (θ = 0°). As it can be assured from the Fig. 3, the extraordinary transmission happens mainly due to non-resonant transmission phenomenon when $t < d$ for PEC, as the EOT angular dependence curve does not depend on structural parameters.

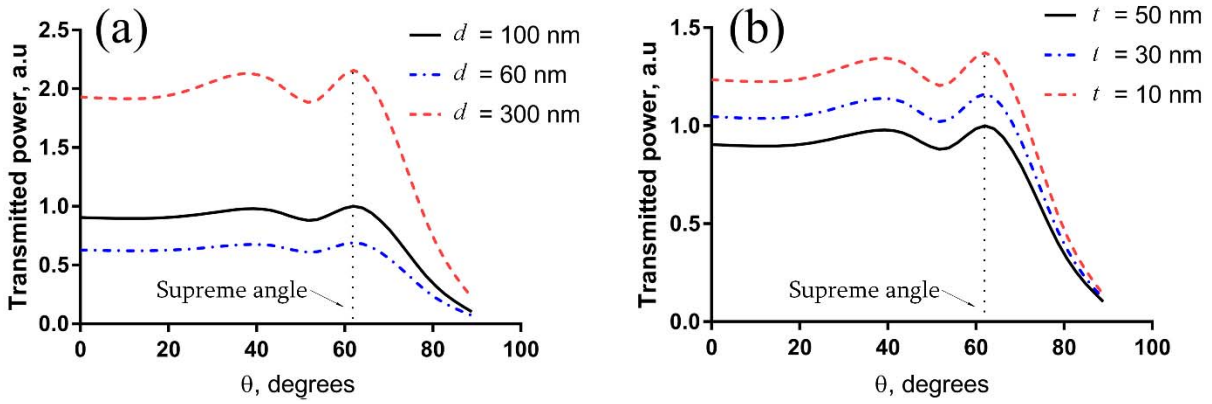

Fig 3. The dependence of normalized transmitted power through the single slit milled in thin Perfect Electric Conductor (PEC) screen on the angle of incidence of a p-polarized wave for 5000 nm wavelength. (a) – when t = 50 nm and slit width d is swept; (b) – when d = 100 nm and metal thickness t is swept. All curves are normalized to the t= 50 nm and d = 100 nm (solid line) curve for reader convenience.

Additionally, we have examined the EOT angular dependence curve for the gold and silver using the refractive indexes provided in [25]. As it was expected, the curves for gold and silver almost perfectly match with PEC curve (Fig. 4), as in the middle infrared region these metals have big enough refractive index to be considered as PECs. Before moving forward, lastly, we analyze the spectral dependence of EOT on incident angle θ in the middle infrared region when $t < d$. As one can notice from Fig.5, the angular dependence behavior is almost the same for a wide range of the spectrum. The only significant difference of curves for various wavelengths is the amount of the transmitted power at any angle, which is in good agreement for the normal incidence [6].

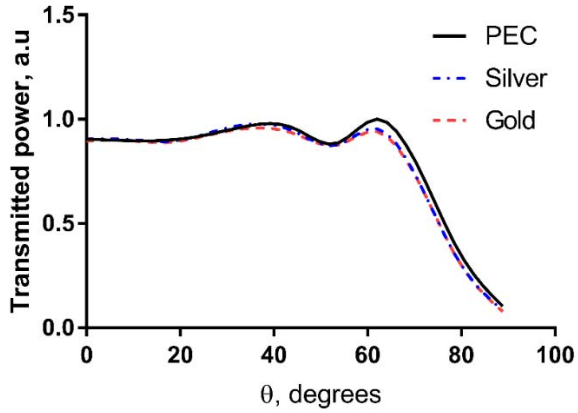

Fig. 4. The dependence of normalized transmitted power through the single slit, milled in the thin metal screen on the angle of incidence of a p-polarized wave for 5000 nm wavelength for gold and silver screens when t = 50 nm, d = 100 nm. All curves are normalized to Perfect Electric Conductor (PEC) curve (solid line).

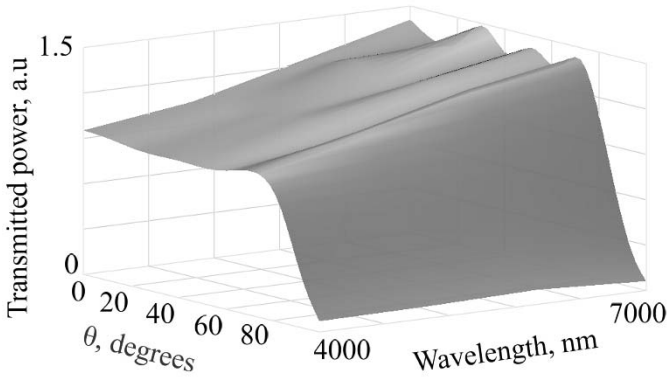

Fig. 5. The dependence of normalized transmitted power through the single slit, milled in the thin Perfect Electric Conductor (PEC) screen on the angle of incidence of a p-polarized wave, when incident wavelength is swept from 4000 nm to 7000 nm. Slit width d = 100 nm and PEC thickness t = 50 nm. Curves for any wavelength are normalized to the curve corresponding to 5000 nm wavelength.

Summing up the above results, it is obvious that transmitted power of non-resonant EOT almost does not depend on the angle of incidence until some supreme angle (near to θ = 62° for PEC in the middle infrared region) after which the transmittance falls to 0. This angle is almost independent of structural sizes and wavelength.

Now, we consider periodic slit structure with p-polarized incidence with wave vector **k** still in the XOY plane (φ = 0, Fig. 1a). The dependence of the transmitted power through the periodic slit system for different *p* periods is presented in Fig. 6. As can be seen, the supreme angle is the same as for

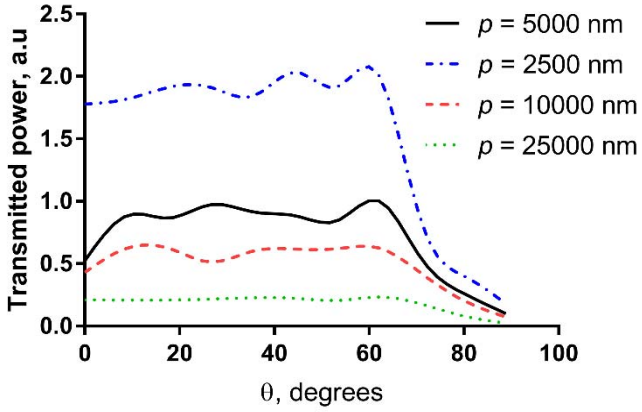

Fig. 6. The dependence of normalized transmitted power through the periodic array of slits, milled in thin Perfect Electric Conductor (PEC) screen on the angle of incidence of a p-polarized wave for 5000 nm wavelength when *t* = 50 nm, *d* = 100 nm for various *p* period of the structure. Curves are normalized to *p* = 5000 nm curve (solid line).

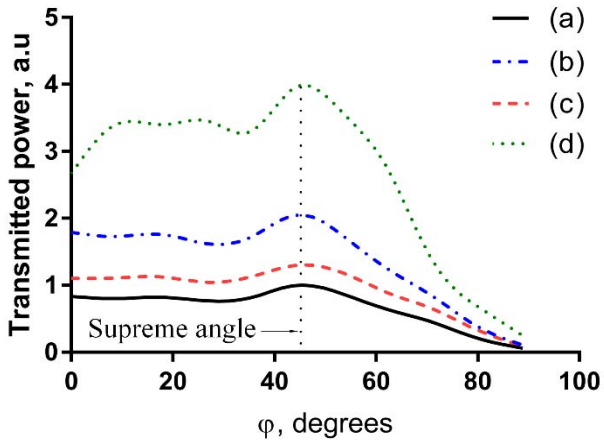

Fig. 7. The dependence of normalized transmitted power through the structure on the angle of incidence of a s-polarized wave on 5000 nm wavelength for (a) single slit, *t* = 50 nm, *d* = 100 nm, (b) single slit, *t* = 50 nm, *d* = 300 nm, (c) single slit, *t* = 10 nm, *d* = 100 nm and (d) *p* = 5000 nm periodic structure of slits, *t* = 50 nm, *d* = 100 nm. All curves are normalized to (a) curve (solid line).

single slit and does not depend on the period as well. So we can assume that this angle is the property of the single slit, namely periodic system helps to enhance transmitted power (as seen in Fig. 6), but does not contribute any change on the supreme angle for non-resonant EOT. For the period of *p* = 25000 nm (five times of incident wavelength) the angular dependence curve (Fig. 5 dotted green line) almost perfectly matches the single slit curve. Therefore, we can think that at these periods slits do not interact with each other and behave as single slits. The resulted curves of the periodic structure in Fig. 6 are in good agreement with the angular dependence curves of [5], calculated using homogenization theory. Lastly, we analyze angular extraordinary transmission through the single slit width d and array of slits milled in thin PEC screen with s-polarized incidence with wave vector **k** in the ZOY plane (θ = 0°, Fig. 1b).

A number of simulations were made for various slit widths *d*, metal thicknesses *t* and structure period's *p* to reveal the s-polarized wave φ angular transmittance curve dependence on these parameters. Overall, the dependence of the transmitted power through the single slit on the incident angle φ is quite similar to the curves in Fig. 3 from the point of view of transmitted power levels but has different supreme angle. To not overload the paper with many graphs we show only four characteristic curves for different slit widths d, PEC thicknesses *t* and structure period *p* in Fig. 7. As

can be seen, the supreme angle is near to φ = 44° and does not depend on slit width *d*, PEC thickness *t* or the period of the structure.

4. Conclusion

Thus, the dependence of non-resonant EOT through a subwavelength slit milled in thin metal screen on the angle of incidence for p- and s-polarized waves was investigated when incident wavelength is much bigger than the slit width. Numerical analysis revealed that transmission intensity dependence on incident angle does not undergo significant changes until its supreme value (62° for the p-polarized wave and 44° for the s-polarized wave) after which intensity falls rapidly. The supreme value of incident angle does not depend on wavelength, slit width, metal screen type or thickness in the wide range of these parameters. It is remarkable that independently of the structural parameters and wavelength, the distribution of transmitted wave fields is represented by the Hankel functions and is homogeneous by angle.

References

[1] T. W. Ebbesen, H. J. Lezec, H. F. Ghaemi, T. Thio, P. A.Wolff, T. Thio, and P. A.Wolff, Nature **86** (1998) 1114.
[2] L. Mart, L. Moreno, F. García-Vidal, Opt. Express. 12 (2004) 3619–28.
[3] C. Genet and T.W. Ebbesen, Nature. 445 (2007) 39–44.
[4] F.J. Garcia-Vidal, L. Martin-Moreno, T.W. Ebbesen, and L. Kuipers, Rev. Mod. Phys. 82 (2010) 729–787.
[5] A. Maurel, S. Félix, J.F. Mercier, Phys. Rev. B - Condens. Matter Mater. Phys. 88 (2013) 1–5.
[6] A. Pors, K. V Nerkararyan, K. Sahakyan, S.I. Bozhevolnyi, Opt. Lett. 41 (2016) 242–5.
[7] N.S. Nye, A.I. Dimitriadis, N. V. Kantartzis, T.D. Tsiboukis, Prog. Electromagn. Res. 143 (2013) 349–368.
[8] F. Fan, S. Chen, S.J. Chang, Int. Conf. Infrared, Millimeter, Terahertz Waves, IRMMW-THz. (2014).
[9] M. Beruete, P. Rodriguez-Ulibarri, V. Pacheco-Peña, M. Navarro-Cia, A.E. Serebryannikov, Phys. Rev. B - Condens. Matter Mater. Phys. 87 (2013).
[10] J. Shu, W. Gao, K. Reichel, D. Nickel, J. Dominguez, I. Brener, D.M. Mittleman, Q. Xu, Opt. Express. 22 (2014) 3747–53.
[11] J.S. White, G. Veronis, Z. Yu, E.S. Barnard, A. Chandran, S. Fan, M.L. Brongersma, Opt. Lett. 34 (2009) 686–8.
[12] M.A. Seo, H.R. Park, S.M. Koo, D.J. Park, J.H. Kang, O.K. Suwal, S.S. Choi, P.C.M. Planken, G.S. Park, N.K. Park, Q.H. Park, D.S. Kim, Nat. Photonics. 3 (2009) 152–156.
[13] B. Hou, Z.H. Hang, W. Wen, C.T. Chan, P. Sheng, Appl. Phys. Lett. 89 (2006) 26–29.
[14] K.L. Van der Molen, F.B. Segerink, N.F. Van Hulst, L. Kuipers, Appl. Phys. Lett. 85 (2004) 4316–4318.
[15] F. Miyamaru and M. Hangyo, Appl. Phys. Lett. 84 (2004) 2742–2744.
[16] M. Beruete, M. Sorolla, I. Campillo, J. S. Dolado, L. Martín-Moreno, J. Bravo-Abad, and F. J. García-Vidal, Opt. Lett. 29 (2004) 2500–2502.
[17] G. D'Aguanno, K.Q. Le, R. Trimm, a. Alù, N. Mattiucci, a. D. Mathias, N. Aközbek, M.J. Bloemer, Sci. Rep. 2 (2012) 1–5.
[18] D. Pacifici, H.J. Lezec, L. a Sweatlock, R.J. Walters, H. a Atwater, Opt. Express. 16 (2008) 9222–9238.
[19] G. Gay, O. Alloschery, B.Viaris de Lesegno, C. O'Dwyer, J.Weiner, and H.J. Lezec, Nat. Phys. 2 (2006) 262.
[20] J. Weiner, Opt. Express 16 (2008) 950-956.
[21] F. Pardo, P. Bouchon, R. Haidar, J.L. Pelouard, Phys. Rev. Lett. 107 (2011).
[22] J. Bravo-Abad, L. Martín-Moreno, F.J. García-Vidal, Phys. Rev. E - Stat. Nonlinear, Soft Matter Phys. 69 (2004) 1–6.
[23] J.R. Suckling, A.P. Hibbins, M.J. Lockyear, T.W. Preist, J.R. Sambles, C.R. Lawrence, Phys. Rev. Lett. 92 (2004) 147401–1.
[24] A. Novitsky, A.M. Ivinskaya, M. Zalkovskij, R. Malureanu, P. Uhd Jepsen, A. V. Lavrinenko, J. Appl. Phys. 112 (2012).
[25] M.A. Ordal, L.L. Long, R.J. Bell, S.E. Bell, R.R. Bell, R.W. Alexander, C.A. Ward, Appl. Opt. 22 (1983) 1099.